Proliferative responses of the TCCs using BLG-derived peptides

The proliferative responses of the TCCs using BLG-derived peptides were assayed as described previously (5). Briefly, the TCCs (3×10^4/well) were cultured in 96-well flat-bottomed culture plates in the presence of BLG-derived analog peptides (1 μM), a soluble BLG peptide mixture (1 μM each), BLG crude protein (25 or 2.5 μg/ml) and 30 Gy-irradiated autologous PBMC (1.5×10^5/well) for 72 h. Before the final 16-h period, 1 μCi per well of [^{3}H]TdR was added, and the incorporated radioactivity was measured by liquid scintillation counting (7).

Production of IL-4, IFN-gamma and IL-10 in supernatants of TCCs using BLG-derived peptides

The TCCs (3×10^4 cells/well in 96-well flat-bottomed culture plates) were cultured in the presence of a soluble BLG peptide mixture (1 μM) and irradiated autologous PBMC (1.5×10^5/well) for 56 hr. Culture supernatants of the TCCs were collected and stored in aliquots at −80°C until the determination of lymphokine concentrations. Enzyme-linked immunosorbent assay kits for detecting human IL-4 (Biosource International), IFN-gamma (Ohtsuka, Tokyo, Japan) and IL-10 (Biosource International) were used for quantification of the lymphokines in the supernatants, according to the manufacturers' instructions.

Binding images between BLGp102-112 and HLA-DRB1*0405 molecules

The binding images between the BLGp102-112 and HLA-DRB1*0405 molecules were displayed with RASMOL, which is the standard molecular graphics program (8).

Results

Intracellular IFN-gamma and IL-4 staining of BLG-specific TCCs

To characterize the TCCs (YA4, HA5.7), intracellular IFN-gamma and IL-4 were analyzed. YA4 showed an intracellular IL-4 single positive cell pattern and HA5.7 showed an IFN-gamma single positive cell pattern (data not shown). These results suggested that YA4 had the Th2 phenotype and HA5.7 had the Th1 phenotype.

Proliferative responses of the TCCs using BLG-truncated peptides

Previously, we reported that the TCCs recognized BLGp97-117 as the core sequence. To define the minimum essential region in BLGp97-117, BLGp97-117 (TDYKKYLLFCMENSAE-PEQSL)-truncated peptides in the N and C termini were designed. The proliferative responses of the TCCs using these truncated peptides were compared (Fig. 1). Although BLGp102-112 (YLLFCMENSAE) induced proliferative responses of TCCs, BLGp103-112 and BLGp102-111 induced no proliferative responses in YA4 and HA5.7. Therefore, both YA4 and HA5.7 recognized BLG p102-112 (YLLFCMENSAE) as the minimal epitope. Proliferative responses and cytokine production of the TCCs using BLG-derived alanine-scan mutant peptides.

To predict the TCR/BLGp102-112/HLA complex structure, BLGp97-117-derived alanine-scan mutant peptides were designed. The proliferative responses of TCCs to pE108A disappeared, and the proliferative responses of TCCs to pC106A decreased (Fig. 2a). The cytokine production patterns are shown in Fig. 2b. In YA4, which had the Th2 phenotype, IL-4 production increased in proportion to its proliferative reaction. In HA5.7, which had the Th1 phenotype, IFN-gamma production increased in proportion to its proliferative reaction. IL-10 production increased according to its proliferative reaction in YA4 and HA5.7 (Fig. 2c).

Proliferative responses and cytokine production of the TCCs using BLG-derived analog peptides

Single amino acid substitution peptides of BLGp102-112 were designed. The proliferative responses of TCCs to these peptides were investigated. pY102S had retained some T-cell responses to both YA4 and HA5.7 (Fig. 3a). pY102S, pL103V and p104V had retained some T-cell responses to HA5.7. IFN-gamma and IL-4 production increased in proportion to their proliferative reaction, as observed in the case of the BLG alanine scan peptide (data not shown). BLG crude induced the IL-10 production of the clones of both YA4 and HA5.7 (Fig. 3b). pY102S showed some IL-10 production of YA4, not HA5.7. pY102S, pL103V, and p104V showed no IL-10 production of HA5.7.

Binding images between BLGp102-112 and HLA-DRB1*0405 molecules

We analyzed that the binding images between the BLGp102-112 and HLA-DRB1*0405 molecules based on the structural modeling. Amino acid residues of L104 and M107 on the BLGp102-112 could be fitted in the pocket of HLA-DRB1*0405 molecules, and F105 and E108 on

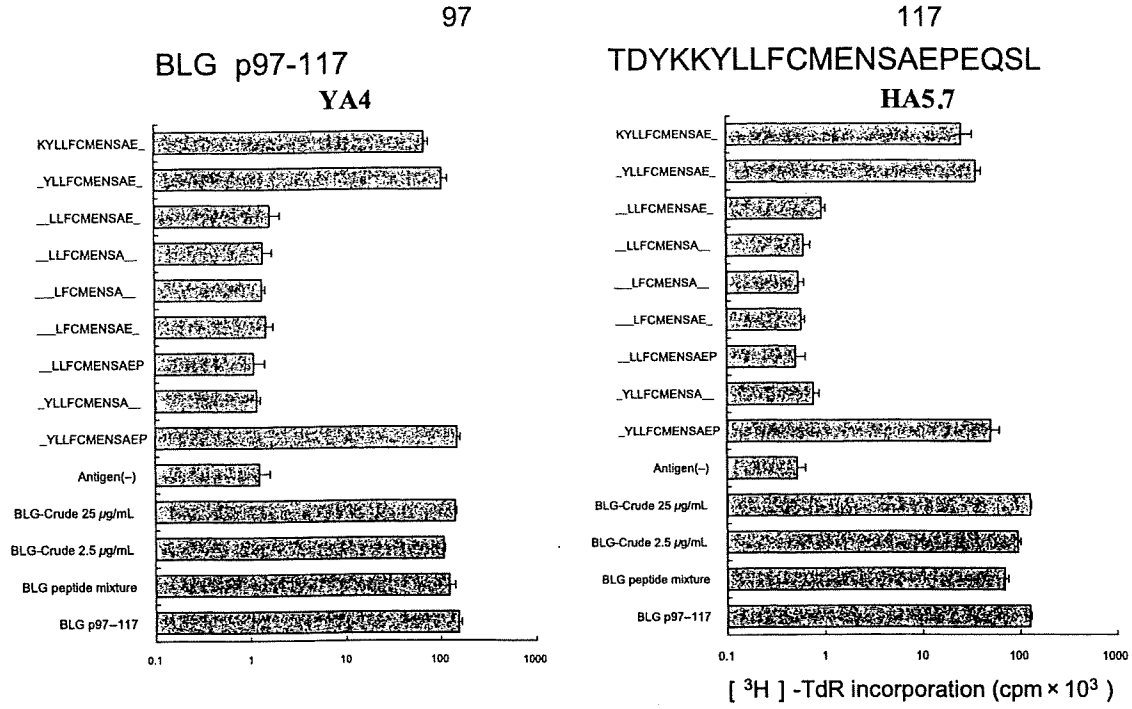

Fig. 1. T-cell clone responses to truncated beta-lactogloulin (BLG) peptides. Peptides truncated from the N- or C-terminal were designed to define the minimal T-cell activation-inducing epitope. The proliferative responses of the TCCs using these truncated peptides are shown. Both TCCs (YA4 and HA5.7) recognized minimal peptide BLGp102-112 (YLLFCMENSAE).

the BLGp102-112 could be presented on the surface of HLA-DRB1*0405 molecules.

CDR3 loops of TCCs (HA5.7) were demonstrated to be 'QKV' in a previous study (6). This sequence is composed of an amide-bearing residue, a positively charged residue, 'K', and a hydrophobic residue, 'Q'. The negatively charged residue, E108, interacted electrically with the 'K' of the CDR3 loops. The hydrophobic residue, F105, and the 'V' of the CDR3 loops interacted with each other (Fig. 4).

Discussion

YA had an immediate type milk allergy and the food challenge test was positive. Her main symptom was urticaria and a skin rash after milk ingestion. HA had immediate and non-immediate type milk allergy. She had atopic dermatitis, a symptom which worsens after milk ingestion. The YA4 clone had a Th2 phenotype and the HA5.7 clone had a Th1 phenotype. In these cases, the clone phenotype was suitable for each clinical symptom. Two TCC (YA4 and HA5.7) needed a minimum of peptide BLGp102-112 (YLLFCMENSAE) presented by HLA-DRB1*0405 to proliferate. By using BLG-derived alanine-scan mutant peptides, the proliferative responses of the TCCs to pE108A disappeared, and those to pC106A decreased. Cytokine secretions of TCCs decreased in proportion to their proliferative responses. Considering the binding images between the BLGp102-112 and HLA-DRB1*0405 molecules based on the structural design reported above, E108 on the BLGp102-112 is the key residue in the proliferation of TCCs.

The major safety concern regarding food allergen immunotherapy has been addressed by engineering 'hypoallergenic' forms of major allergenic food proteins. These mutated ('engineered') major food proteins have lost their ability to bind to IgE but have retained the ability to interact with T cells (9). In previous literature, the tolerogenic peptide size is around 20 amino acids (10–14). These tolerogenic peptide sizes are in accord with the fact that peptides with 12 to 20 amino acids presented with HLA complex class II molecules on the surface of antigen-presenting cells are recognized by T cells (15). The presence of T-cell epitopes is essential for tolerogenic peptides as immunomodulation is mainly induced by T cells (16). In our cases, the analog peptides that change amino acids pY102A and pY102S have some T-cell response to TCCs. pY102A induced some IL-10 production in YA4

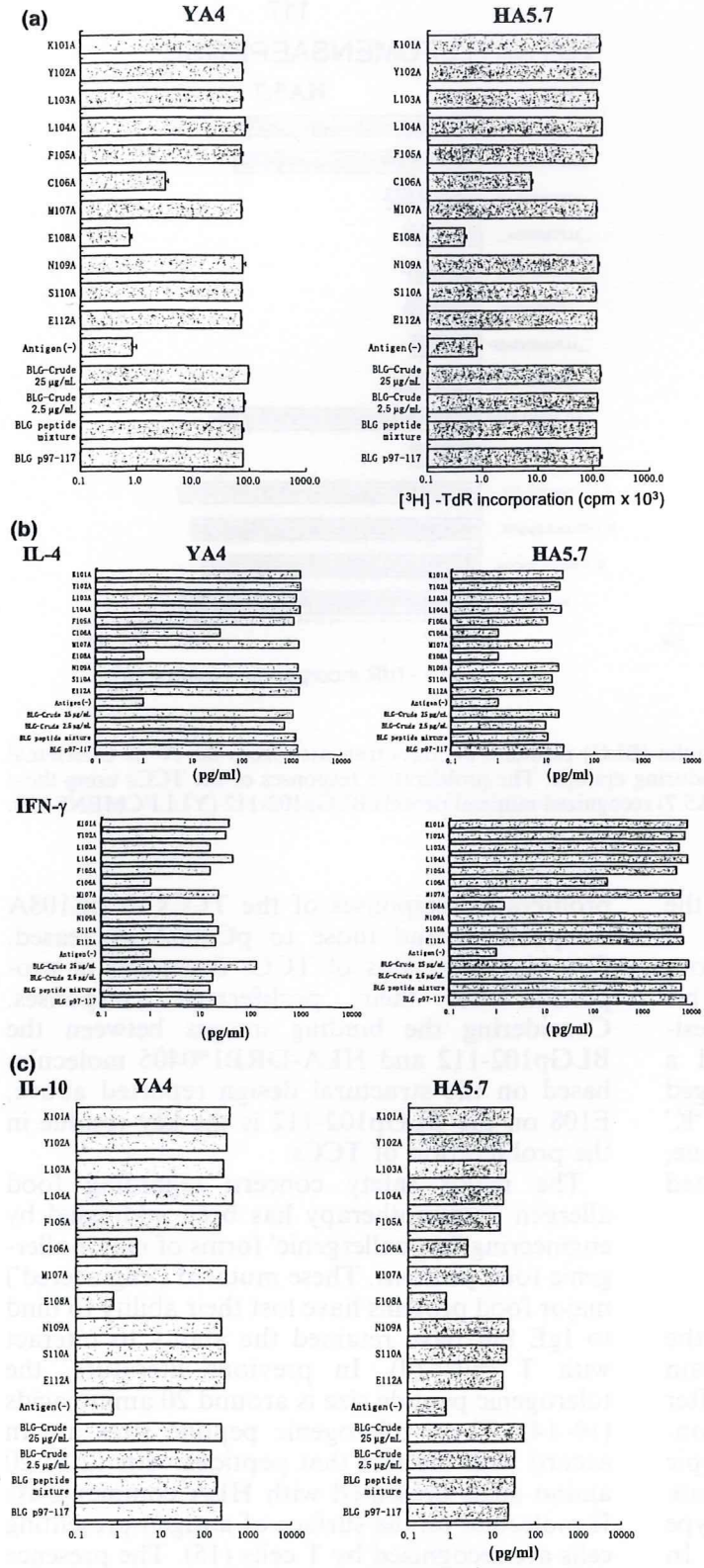

Fig. 2. T-cell clone (TCC) responses to beta-lactoglobulin (BLG) alanine-scan mutant peptides. BLGp97-117-derived alanine-scan mutant peptides were designed. Each polypeptide has 21 amino acid residues from number 97 to 117 and contains one amino acid substitution for alanine. The BLG peptide mixture is a mixture of synthetic peptides composed of 12-21 residues overlapping each other by 11 residues (5). BLG crude is a BLG protein (25 or 2.5 μg/ml). (a) The proliferative responses of the TCCs against BLGp97-117-derived alanine-scan mutant peptides were shown. (b) IL-4 and IFN-gamma production of the TCCs against BLGp97-117-derived alanine-scan mutant peptides was shown. (c) IL-10 production of the TCCs against BLGp97-117-derived alanine-scan mutant peptides was shown.

(Fig. 3b). It has been reported that IL-10 induced T-cell anergy and played an important role in the induction and maintenance of antigen-specific T-cell tolerance (17). These results show that pY102A and pY102S might have potential as immunoregulatory peptides.

In this study, alanine-scan was performed because it lacks the side chain of the native

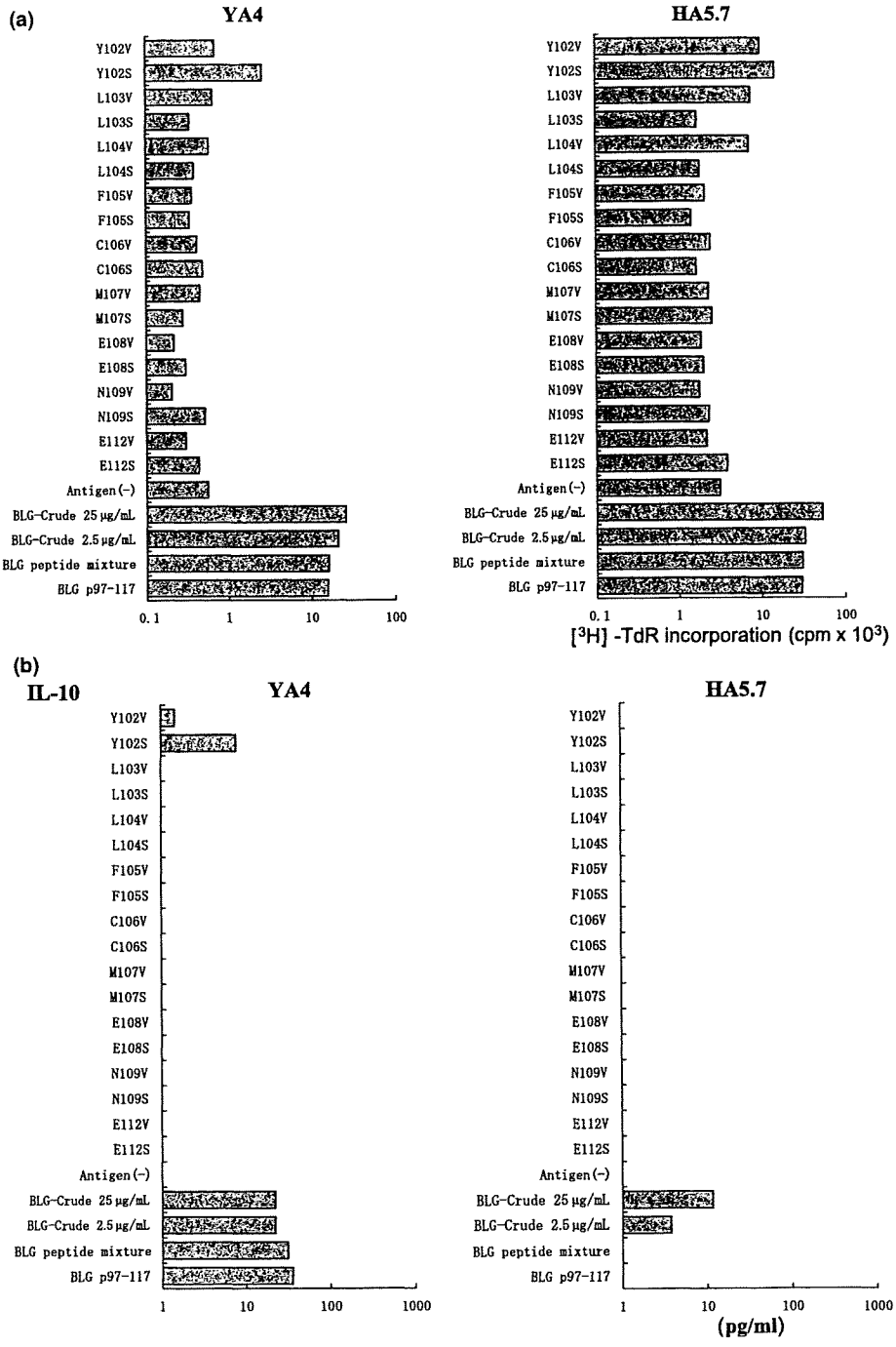

Fig. 3. T-cell clone (TCC) responses to beta-lactoglobulin (BLG) analog peptides. Single amino acid substitution peptides of BLGp102-112 were designed. Each polypeptide has 11 amino acid residues from number 102 to 112 and contains one amino acid substitution, as indicated in Fig. 3. (a) Proliferative responses of the TCCs to single amino acid-substituted peptides of BLG p102-112 are shown. (b) IL-10 production of the TCCs to single amino acid-substituted peptides of BLG p102-112 is shown.

amino acid beyond the β carbon and thus can assess the impact of its absence on binding affinity. It does not alter significantly the main-chain conformation and does not impose extreme electrostatic or steric effects.

In conclusion, this study has identified the T-cell minimal core epitope, predicted the TCR/BLG-peptide/HLA complex structure, and searched for the immunomodulated peptides. The p105-108 substitutions are important to retain the TCR/BLG-peptide/HLA complex structure. Our data suggest that peptides with a mutated core epitope might be considered as candidate peptides for the modification

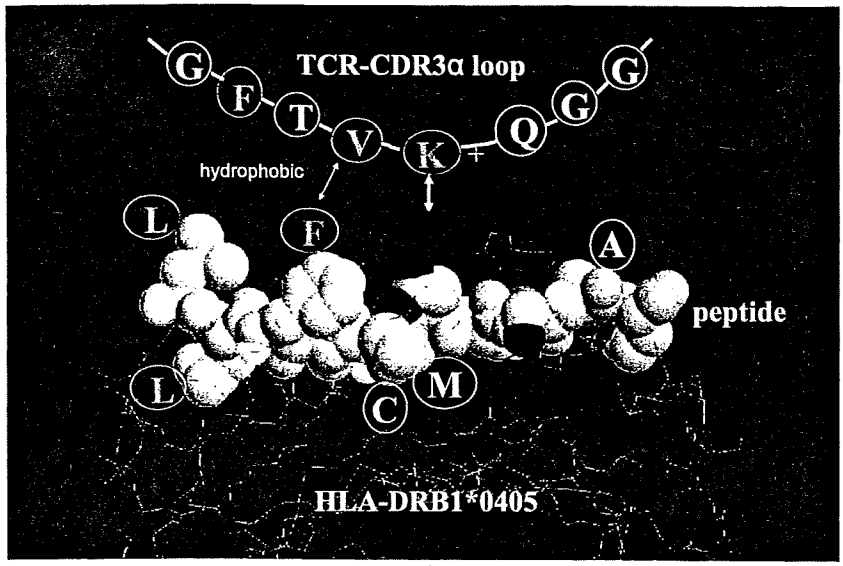

Fig. 4. Binding images between BLGp102-112 and HLA-DRB1*0405 molecules based on structural modeling. The CDR3 loops of the TCCs (HA5.7) were demonstrated to be 'QKV'. The negatively charged residue pE108 and the positively charged residue 'K' of the CDR3 loops interacted. The hydrophobic residue pF105 and 'V' of the CDR3 loops interacted with each other.

of the T-cell response to BLG in cow's milk allergy.

Acknowledgments

This study was in part funded by the Research and Development Program for New Bio-industry Initiatives (2005–2009) of the Bio-oriented Technology Research Advancement Institution (BRAIN), Japan.

References

1. Saarinen KM, Juntunen-Backman K, Jarvenpaa AL, et al. Supplementary feeding in maternity hospitals and the risk of cow's milk allergy: A prospective study of 6209 infants. J Allergy Clin Immunol 1999: 104: 457–61.
2. Sampson HA. Food allergy. Part 1: immunopathogenesis and clinical disorders. J Allergy Clin Immunol 1999: 103: 717–28.
3. Wal J-M. Cow's milk allergens. Allergy 1998: 53: 1013–22.
4. Selo I, Clement G, Bernard H, et al. Allergy to bovine beta-lactoglobulin: specificity of human IgE to tryptic peptides. Clin Exp Allergy 1999: 29: 1055–63.
5. Inoue R, Matsushita S, Kaneko H, et al. Identification of beta-lactoglobulin-derived peptides and class II HLA molecules recognized by T cells from patients with milk allergy. Clin Exp Allergy 2001: 31: 1126–34.
6. Sakaguchi H, Inoue R, Kaneko H, et al. Interaction among human leucocyte antigen-peptide-T cell receptor complexes in cow's milk allergy: the significance of human leucocyte antigen and T cell receptor-complementarity determining region 3 loops. Clin Exp Allergy 2002: 32: 762–70.
7. Kondo N, Agata H, Fukutomi O, Motoyoshi F, Orii T. Lymphocyte responses to food antigens in patients with atopic dermatitis who are sensitive to foods. J Allergy Clin Immunol 1990: 86: 253–60.
8. Sayle RA, Milner-White EJ. RASMOL: biomolecular graphics for all. Trends Biochem Sci 1995: 20: 374.
9. Ferreira F, Ebner C, Kramer B, et al. Modulation of IgE reactivity of allergens by site-directed mutagenesis: potential use of hypoallergenic variants for immunotherapy. FASEB J 1998: 12: 231–42.
10. Bousquet J, Becker WM, Hejjaoui A, et al. Differences in clinical and immunologic reactivity of patients allergic to grass pollens and to multiple-pollen species. II. Efficacy of a double-blind, placebo-controlled, specific immunotherapy with standardized extracts. J Allergy Clin Immunol 1991: 88: 43–53.
11. Pecquet S, Bovetto L, Maynard F, Fritsche R. Peptides obtained by tryptic hydrolysis of bovine beta-lactoglobulin induce specific oral tolerance in mice. J Allergy Clin Immunol 2000: 105: 514–21.
12. Fritsche R, Pahud JJ, Pecquet S, Pfeifer A. Induction of systemic immunologic tolerance to beta-lactoglobulin by oral administration of a whey protein hydrolysate. J Allergy Clin Immunol 1997: 100: 266–73.
13. Ferguson TA, Peters T Jr, Reed R, Pesce AJ, Michael JG. Immunoregulatory properties of antigenic fragments from bovine serum albumin. Cell Immunol 1983: 78: 1–12.
14. Litwin A, Pesce AJ, Fischer T, Michael M, Michael JG. Regulation of the human immune response to ragweed pollen by immunotherapy. A controlled trial comparing the effect of immunosuppressive peptic fragments of short ragweed with standard treatment. Clin Exp Allergy 1991: 21: 457–65.
15. Rudensky AYu, Preston-Hurlburt P, Hong SC, Barlow A, Janeway CA Jr. Sequence analysis of peptides bound to MHC class II molecules. Nature 1991: 353: 622–7.
16. Hoyne G, Callow M, Kuo M, Thomas W. Inhibition of T-cell responses by feeding peptides containing major and cryptic epitopes: studies with the Der p1 allergen. Immunology 1994: 83: 190–5.
17. Groux H, Bigler M, de Vries JE, Roncarolo MG. Interleukin-10 induces a long-term antigen-specific anergic state in human CD4+ T cells. J Exp Med 1996: 184: 19–29.

Allergology International. 2009;58:111-117
DOI: 10.2332/allergolint.O-08-549

ORIGINAL ARTICLE

Various Expression Patterns of α1 and α2 Genes in IgA Deficiency

Hiroko Suzuki[1], Hideo Kaneko[1], Toshiyuki Fukao[1], Rong Jin[1], Norio Kawamoto[1], Tsutomu Asano[1], Eiko Matsui[1], Kimiko Kasahara[1] and Naomi Kondo[1]

ABSTRACT

Background: IgA deficiency (IgAD) is the most common immunodeficiency, however the pathogenesis in most cases of IgAD is unknown. There are 2 subclasses of IgA, IgA1 and IgA2, and its heavy chains are encoded by 2 different genes, the α1 and α2 genes. To investigate the molecular pathogenesis of IgA deficiency, it is important to evaluate each of the expressions of IgA1 and IgA2 separately.

Methods: In this study, we report on the reverse transcriptase (RT)-PCR method in which α1 and α2 mRNAs can be separately evaluated. This method is based on electrophoretic separation using the difference of 39 bases between α1 and α2 mRNAs. Three selective, 5 partial and 2 secondary IgAD patients were examined.

Results: In the 3 selective IgAD patients, no α1 or α2 mRNA expression was detected. In the 5 partial IgAD patients, various α1 and α2 mRNA expression patterns were found. One of the partial IgAD patients showed only α2 gene expression, but not α1 gene expression, and was found to show an α1 gene deletion together with γ2 and ε gene deletions. His plasma IgA2 level was within the normal range.

Conclusions: Patients with an α1 gene deletion can be considered as having partial IgAD. Using this method, we identified the second case of α1 gene deletion in Japan, and classified IgAD patients on the basis of α1 and α2 expression.

KEY WORDS

gene expression, IgA subclasses, partial IgA deficiency, selective IgA deficiency, α1 gene deletion

ABBREVIATIONS

IgA, immunoglobulin A; IgAD, immunoglobulin A deficiency; RT, reverse transcriptase; CVID, common variable immunodeficiency; TACI, transmembrane activator and calcium-modulator and cyclophilin ligand interactor; SD, standard deviation; PBMCs, peripheral blood mononuclear cells; GAPDH, glyceraldehyde-3-phosphate dehydrogenase; ELISA, enzyme-linked immunosorbent assay; HRP, horseradish peroxidase; BSA, bovine serum albumin; PBS, phosphate-buffered saline

INTRODUCTION

Human immunoglobulin A (IgA) is the most abundant immunoglobulin in secretions. IgA has 2 subclasses, IgA1 and IgA2. The ratios of IgA1 : IgA2 are approximately 9 : 1 in serum and 6 : 4 in saliva.[1] In mucosal tissue, IgA synthesis greatly exceeds that of other immunoglobulin classes. These 2 subclasses play important roles in the first line of defense, and the amount ratio of these molecules in secretions varies.

Selective IgA deficiency (IgAD) is the most common immunodeficiency, and has been found with a frequency ranging from 0.03 to 0.3%. The prevalence differs according to ethnic groups, with a lower frequency in the Japanese population, namely, 1/18,000 people.[2,3] Most IgAD patients remain healthy, but some suffer from a variety of infections, allergies, autoimmune disorders, gastrointestinal diseases, malignancies, endocrinopathies, neurological diseases, and genetic disorders.[2,4] The pathogenesis of IgAD has not yet been completely clarified. IgAD has been found to be associated with IgG2, IgG4, and IgE deficiencies.[5-8] The class switch disorder in IgA-producing B lymphocytes is one of the most important factors in IgAD patients.[9] Asano *et al.* suggested

[1]Department of Pediatrics, Graduate School of Medicine, Gifu University, Gifu, Japan.
Correspondence: Hiroko Suzuki, Department of Pediatrics, Graduate School of Medicine, Gifu University, 1-1 Yanagido, Gifu 501-1194, Japan.
Email: hori_hiro2002@yahoo.co.jp
Received 11 March 2008. Accepted for publication 29 July 2008.

Table 1 Immunological data of patients

Patient No.	Sex	Age	Serum level (mg/dl)			IgG subclass (mg/dl)			
			IgG	IgA	IgM	IgG1	IgG2	IgG3	IgG4
Selective IgA deficiency									
1	M	10 years	1363	< 5	146	619	255	57.3	33.9
2	F	11 years	1640	< 5	117	949	400	47.7	90.2
3	F	17 years	1261	< 5	137	630	625	35.1	18.4
Partial IgA deficiency									
4	M	4 years	1223	17	120	933	< 8.0	22.8	< 3.0
5	F	3 years	1644	15	150	878	47.9	17.3	32.1
6	F	3 years	869	27	106	306	69.3	27.6	3.8
7	M	4 years	887	45	101	295	97.0	40.0	4.4
8	M	4 years	1624	8	100	1090	120	74.7	< 3.0
Secondary IgA deficiency									
9	F	7 years	913	12	105	602	148	52.8	16.5
10	M	13 years	705	9	39	852	345	49.8	6.4

that decreased expression levels of Iα germline transcripts before a class switch may be the cause of selective IgAD, and B-cell differentiation might be disturbed after a class switch in partial IgAD patients.[10] Husain *et al.* reported that the increased destruction of a subset of B cells is the cause for the inability to produce IgA in IgAD patients.[11]

The association between IgAD and common variable immunodeficiency (CVID) has been discussed,[3] and it was reported recently that some CVID and IgAD patients have mutations in TNFRSF13B (encoding TACI; transmembrane activator and calcium-modulator and cyclophilin ligand interactor).[12,13]

The molecular weights of the IgA1 and IgA2 heavy chains are both approximately 53 kD. The α1 and α2 genes show about 97% of its identity.[14] This high homology between them makes it difficult to analyze the α1 and α2 genes separately. The α-chain constant region of both α1 and α2 genes is encoded by 3 exons. The hinge region of the human α chain is encoded at the beginning of the second exon. The hinge region of the α2 gene shows a deletion of 39 nucleotides (corresponding to 13 amino acids) when compared with that of the α1 gene.[1,15] To clarify the pathogenesis and immunological reactions of IgAD clear, we analyzed α1 and α2 gene expression in IgAD patients. In this study, we devised a new method to determine the expression levels of the α1 and α2 genes, and analyzed selective, partial and secondary IgAD patients.

METHODS

SUBJECTS

As shown in Table 1, we analyzed 3 selective IgAD patients (patients number 1, 2 and 3) with serum IgA levels below the detection limit (<5 mg/dl), 5 partial IgAD patients (patients number 4, 5, 6, 7, and 8) with serum IgA levels above 5 mg/dl but having more than 2 standard deviations (SDs) below the normal level, and 2 secondary IgAD patients (patients number 9 and 10) whose conditions were caused by epileptic medication. Ten controls were also included in this study. Two of the 10 controls were child volunteers under 16 years of age, and the other 8 were adult volunteers 16 years or older. We obtained informed consent from the patients, controls, and parents of minors.

CELL PREPARATION

Peripheral blood mononuclear cells (PBMCs) were collected in heparin and separated by gradient centrifugation in Ficoll-Paque (GE Healthcare Bio-Sciences AB, Uppsala, Sweden).[16] The cells were suspended at a density of 10^6/ml and incubated for 24 hours in RPMI 1640 medium supplemented with 10% heat-inactivated fetal calf serum, 2 mmol/l l-glutamine, 100 U/ml penicillin and 100 μg/ml streptomycin.[10] In comparison with non-cultured cells, cells cultured for 24 hours showed higher levels of α1 and α2 gene expression (unpublished data).

cDNA SYNTHESIS AND PCR AMPLIFICATION

We extracted total RNA from PBMCs using an Isogen kit (Nippon Gene, Tokyo, Japan), and cDNA synthesis was carried out using 1 or 2 μg of total RNA with oligo-dT and M-MLV reverse transcriptase (Invitrogen, Carlsbad, CA, USA). We used the following PCR primer pair, which was targeted to the common sequence area of the α1 and α2 genes: sense 5'-CCTGGTCACCGTCTCCTCA-3' (placed at the J exon; Gene Bank accession number-L20778) and antisense 5'-TCACGCTCAGGTGGTCCTTG-3' (placed at the Cα CH2 exon)[17] (Fig. 1A). The PCR fragments included the CH1, hinge and CH2 regions, and the size was 532 bp for the α1 gene and 493 bp for the α2 gene. The PCR program was 35 or 40 cycles of 94℃

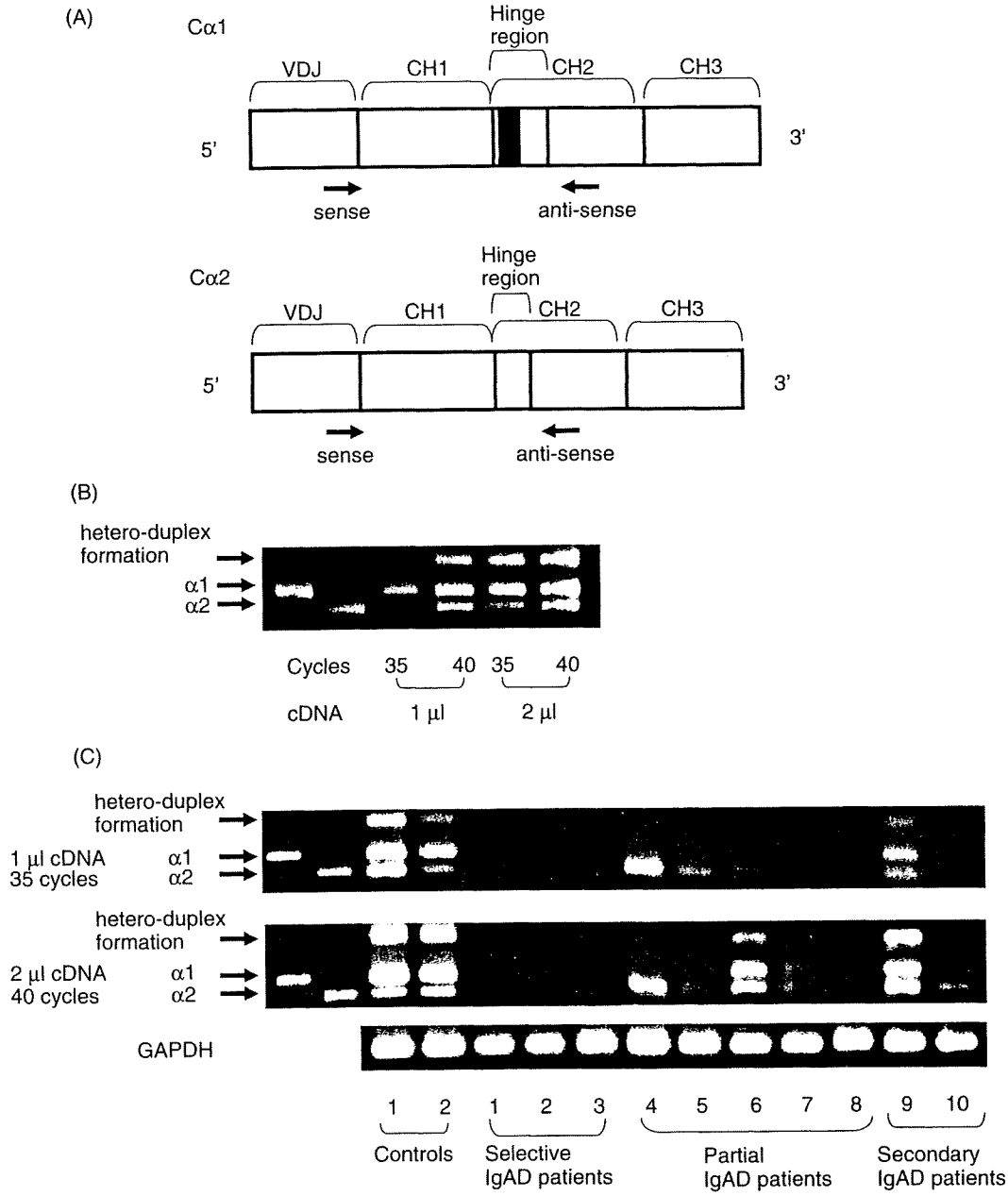

Fig. 1 Structure and expression of the α1 and α2 genes. (**A**) The primer pair was targeted to the common sequence area of the α1 and α2 genes. These figures show mature Cα gene transcripts. The arrows indicate the positions of the primers. The black box indicates the deletion of 39 bases. VDJ: variable diversity joining region, CH: constant heavy chain. (**B**) RT-PCR analysis of RNA extracted from the PBMCs of a control subject, starting from 1 μl or 2 μl of cDNA and using 35 or 40 cycles. The two lanes at the left show PCR products amplified from the template DNA, which are T-vectors containing the IgA1 (lane 1) or IgA2 (lane 2) genes. (**C**) RT-PCR analysis of RNA extracted from the PBMCs of control subjects and IgAD patients. The α1 fragment, α2 fragment, and hetero-duplex formation are indicated by arrows. GAPDH was used as a control.

for 1 minute, 60℃ for 1 minute, and 72℃ for 1 minute using 1 or 2 μl of cDNA. The PCR products were run on 4% agarose gels for 120 minutes. Glyceraldehyde-3-phosphate dehydrogenase (GAPDH) was used as a control.

DNA EXTRACTION AND PCR AMPLIFICATION

Genomic DNA was purified from polymorphonuclear

cells using Sepa Gene (Sanko Junyaku, Tokyo, Japan). We used the following PCR primer pair, which was targeted at the common sequence area of the α1 and α2 genes: sense 5'-TGACCAGCTCAGGCCATCT CT-3' and antisense 5'-CTTTGCAAACCAGAGCACT GA-3'. The PCR program was 40 cycles of 94℃ for 1 minute, 58℃ for 1 minute, and 72℃ for 1 minute. Four percent agarose gel electrophoresis was performed for 120 minutes. The other primer pairs were as follows: for amplification of the Cε gene, sense 5'-A CCTTCAGCGGTAAGAGAGGG-3' and antisense 5'-T GGGAACGTACCTGCACACTT-3', (the PCR program was 35 cycles of 94℃ for 1 minute, 60℃ for 1 minute, and 72℃ for 1 minute); for amplification of the Cγ2 gene, sense 5'-ATCTCTTCCTCAGCACCACCT-3' and antisense 5'-CGTGGCACTCATTTACCCGGA-3', (the PCR program was 35 cycles of 94℃ for 1 minute, 58 ℃ for 1 minute, and 72℃ for 1 minute); for the Cμ gene, sense 5'-ATGTGTGTCCCCGGTGAGTGA-3' and antisense 5'-AGGGCCACCCCTGTGAACAGA-3', (the PCR program was 35 cycles of 94℃ for 1 minute, 58℃ for 1 minute, and 72℃ for 1 minute).

QUANTIFICATION OF IgA SUBCLASSES IN PLASMA

The levels of the IgA subclasses in plasma were measured by enzyme-linked immunosorbent assay (ELISA). For IgA1, coating was performed with a mouse monoclonal anti-IgA1 (NI69-11), and detection of IgA1 was performed with horseradish peroxidase (HRP)-labeled goat anti-human IgA (Cappel, Organon Teknika, Turnhout, Belgium).[18] For IgA2, coating was performed using goat anti-human IgA (BETHYL, Montgomery, TX, USA), and detection of IgA2 was performed using mouse anti-human IgA2-HRP (B3506B4).[19] ELISA plates were coated overnight at 4 ℃ with mouse monoclonal anti-IgA1 (diluted to 1 : 200 with 0.05 M sodium carbonate, pH 9.6) or goat anti-human IgA (diluted to 1 : 100 with 0.05 M sodium carbonate, pH 9.6). The plates were washed then incubated with standard serum and plasma dilutions. IgA1 was detected using goat anti-human IgA-HRP (diluted to 1 : 10000 with 1% bovine serum albumin [BSA] in phosphate-buffered saline [PBS]-0.02% Tween 20), and IgA2 was detected using mouse anti-human IgA2-HRP (diluted to 1 : 1000 with 1% BSA in PBS-0.02% Tween 20). The samples were tested repeatedly. The lower limits of IgA1 and IgA2 detection were 5 ng/ml and 1 μg/ml, respectively.

RESULTS

PCR AMPLIFICATION OF α1 AND α2 GENE EXPRESSION

RT-PCR analysis was performed using primer pairs that amplified both α1 and α2 mRNAs and could distinguish α2 mRNA from α1 mRNA taking advantage of the deletion of 39 bases in the hinge region of the α2 gene. Various PCR conditions were tested, and the optimal conditions were deemed to be 2 μl of cDNA and 40 cycles of amplification (Fig. 1B). Control samples gave an intense α1 band and a less-intense, shorter α2 band in all 4 PCR conditions. Another band with less electrophoretic mobility than the α1 band was determined to be a hetero-duplex formation of the α1 and α2 fragments, because the subcloning of this band yielded clones of the α1 and α2 fragments. Figure 1C shows α1 and α2 gene expression in 10 IgAD patients. In 3 selective IgAD patients (patients number 1, 2 and 3), no expression of the α1 and α2 genes was detected. Three partial IgAD patients (patients number 5, 6 and 7) and 2 secondary IgAD patients (patients number 9 and 10) showed α2 and α1 gene expressions; however, patient No. 4 showed only α2 gene expression, but no α1 gene expression. One partial IgAD patient (No. 8) showed no bands in this RT-PCR analysis.

PLASMA IgA LEVELS IN CONTROLS AND IgAD PATIENTS

Plasma IgA1 and IgA2 levels were assayed separately (Table 2). The IgA1 levels were much higher than the IgA2 levels in the 10 controls. In the 3 selective IgAD patients, plasma IgA1 and IgA2 levels were very low. One partial IgAD patient (patient No. 4) had a normal IgA2 level, but no detectable IgA1. This finding is in accordance with the result of this patient showing no α1 gene expression in PBMCs. Although the IgA2 level of patient No. 5 was below the threshold, other patients with partial IgAD (patients number 6, 7, 8) showed various IgA1 and IgA2 levels although these levels were much lower than that of the control group.

PCR AMPLIFICATION OF THE IMMUNOGLOBULIN GENES OF IgAD PATIENTS

In patient No. 4, α1 gene expression was not detected and no IgA1 protein was detected in his plasma. As shown in Table 1, the plasma levels of the IgG subclasses showed that IgG2 and IgG4 levels were below the detection limits. Hence, we carried out PCR amplification of the genomic α2 and α1 genes, together with the μ, γ2 and ε genes. As shown in Figure 2, no PCR products were detected for the α1, γ2 and ε genes in patient No. 4, whereas they were clearly be detected in 2 control and other IgAD patients. A large genomic deletion of the A1-GP-G2-G4-E genes can be proposed as the molecular basis of IgAD in patient No. 4.

LONGITUDINAL CHANGE IN THE SERUM IgA LEVEL OF PATIENT NO. 4

The immunological data of 2 families of patients with IgG2-IgG4-IgA1-IgE deficiency, including patient No. 4, are shown in Table 3. The serum IgA levels of patient No. 4 over time are shown in Table 4. The patient's IgA levels remained at a level more than 2 SDs

Table 2 The levels of IgA subclasses and IgA1/IgA2 ratios in plasma as measured by ELISA

Patient No.	Serum IgA levels (mg/dl)	Plasma IgA1 and IgA2 levels (mg/dl)		IgA1/IgA2 ratio	mRNA expression		Genes	
		IgA1	IgA2		α1	α2	α1	α2
Selective IgA deficiency								
1	< 5	2.48 ± 0.26	ND†	NC‡	−¶	−	+§	+
2	< 5	ND	ND	NC	−	−	+	+
3	< 5	2.16 ± 0.74	ND	NC	−	−	+	+
Partial IgA deficiency								
4	17	ND	13.67 ± 1.39	NC	−	+	−	+
5	15	2.71 ± 0.36	ND	NC	+	+	+	+
6	27	8.28 ± 0.52	0.91 ± 0.25	8.40	+	+	+	+
7	45	29.29 ± 6.83	4.88 ± 0.54	6.97	+	+	+	+
8	8	6.28 ± 0.67	0.86 ± 0.45	8.87	−	−	+	+
Secondary IgA deficiency								
9	12	8.59 ± 1.77	1.17 ± 0.36	6.56	+	+	+	+
10	9	0.56 ± 0.09	0.18 ± 0.03	3.03	+	+	+	+
Controls (n = 10)		128.02 ± 36.98	19.39 ± 8.93	7.96 ± 4.14				

† ND : undetected, ‡ NC : not calculated.
§ + : detected, ¶ − : undetected.

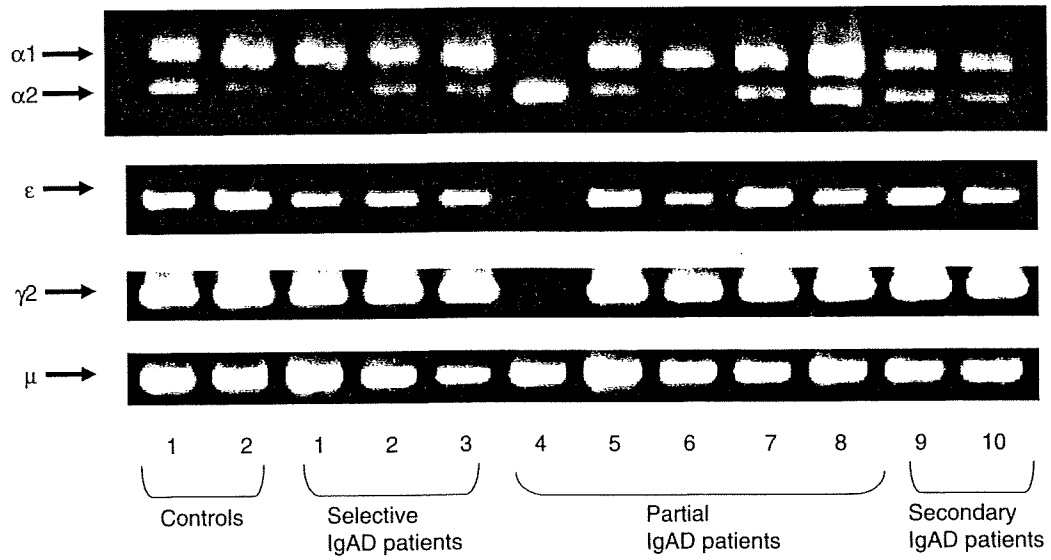

Fig. 2 PCR analysis of immunoglobulin genes in IgAD patients. PCR analysis of α1, α2, ε, γ2 and μ genes was performed in control subjects and IgAD patients. Two different sized bands for the α gene appeared, corresponding to the α1 and α2 genes, as indicated by arrows.

below the normal value, but above 5 mg/dl. The immunological data of his family members are shown in Family 1 (Table 3). The patient's older brother was also found to have the same gene deletion. His serum IgA level was 21 mg/dl, and he also showed a pattern of partial IgAD. The serum IgA levels of another patient with IgG2-IgG4-IgA1-IgE deficiency and her family members are shown as Family 2 (Table 3).[8] Both the patient and her older sister had the same deletions of the A1-GP-G2-G4-E genes. The serum IgA level of the patient's sister was 18 mg/dl and she also showed a pattern of partial IgAD.

DISCUSSION

The serum IgA subclass levels of IgAD patients, particularly selective IgAD patients, are very difficult to measure by ELISA; thus, there have been few reports on the levels of serum IgA subclasses in IgAD patients. The α1 and α2 gene expression levels are low in most IgAD patients, and there have been no previous reports on the gene expression levels of the IgA subclasses in these patients.[20-23] Hummelshoj *et al.*

Table 3 Immunological data of patient no. 4 and 2 families of patients with IgG2-IgG4-IgA1-IgE deficiency

Family 1							
	Age	Serum level					
		mg/dl					IU/ml
		IgA	IgG1	IgG2	IgG3	IgG4	IgE
Patient No. 4	4	17	933	< 8.0	22.8	< 3.0	< 2.0
Father	45	119	659	451	58.0	19.0	70.0
Mother	41	201	730	224	25.4	14.2	190.0
Brother	11	21	952	< 8.0	23.3	< 3.0	< 2.0
Family 2							
	Age	Serum level					
		mg/dl					IU/ml
		IgA	IgG1	IgG2	IgG3	IgG4	IgE
Patient	1	< 5	996	< 8.0	10.4	< 3.0	< 5.0
Father	27	161	720	281	13.7	14.1	214.8
Mother	26	180	794	248	16.7	8.2	4.2
Sister	3	18	645	< 8.0	15.1	< 3.0	< 5.0

Table 4 Longitudinal change in the serum IgA levels of patient no. 4

	20m	25m	30m	38m	56m	57m
Serum IgA level (mg/dl)	11	12	11	11	20	17
Normal value†	1year	2y		3y	4y	
Mean (±2SD)	49 (16-128)	60 (20-149)		74 (25-174)	89 (31-202)	

† data on normal values according to reference 28.

reported on the expression of germline transcripts of the α1 and α2 genes in IgAD patients.[24] The germline transcripts were induced during stimulation with TGF-β, however their levels were lower than those of control subjects. Our report shows the expression of mature transcripts of the α1 and α2 genes in partial IgAD patients. In the 3 selective IgAD patients, no expression of α1 and α2 genes was detected, presumably because the expression level was too low. In 2 of them, only plasma IgA1 levels could be measured, and in 1 of them, neither IgA1 nor IgA2 levels were unable to be measured. Patient No. 8 showed no mRNA expression of IgA subclasses, but exhibited detectable levels of plasma IgA1 and IgA2 levels. It might be assumed that the pathogenesis of partial IgAD in patient No. 8 is similar to that in selective IgAD patients. As shown in Table 2, patients number 1, 2, 3 and 8 showed no α1 or α2 gene expression, while patients number 5, 6, 7, 9 and 10 showed both α1 and α2 gene expression. There is a possibility that the mechanism underlying IgA deficiency may be different between these 2 groups. The plasma IgA2 levels were unable to be measured in 1 partial IgAD patient; however, α2 gene expression was seen in this patient using our method. This method is effective for determining whether partial IgAD patients lack expression of the α1 and α2 genes when their plasma IgA, IgA1 and IgA2 levels are under the detection limit.

Asano *et al.* reported detectable levels of the Cα mature transcripts by RT-PCR using the same sense primer we employed and an antisense primer located in the Cα CH1 region.[10] Using our method, no α1 or α2 gene expression was detected in 3 selective IgAD patients. There was a difference in the annealing temperatures used (59℃ in the study of Asano *et al.*), and different PCR conditions may result due to changes in the sensitivity of the assay.

IgAD patients are often associated with IgG subclass deficiency. In our study, 2 IgAD patients (patients number 4 and 8) had IgG subclass deficiency in the serum. Patient No. 4 showed deletions of the γ2 and ε genes, and was considered to have a large genomic deletion of the Cα1, ΨCγ, Cγ2, Cγ4 and Cε genes, showing the same observations reported previously in a patient.[8] In Japan, only 1 case has ever been reported. Beard *et al.*[25] reported that IgA-IgG2-IgG4 deficiency occurs in 4% of 73 IgAD patients. Deletions of the A1-GP-G2-G4-E genes are the most common deletions of the Ig heavy chain locus.[26] There could be more patients with an α1 gene deletion who might have partial IgAD. Partial IgAD is

often transient,[27] however, patients who have a deletion of the α gene will not show transient IgAD and will exhibit continuous partial IgAD.

We also classified the IgAD patients on the basis of the expression of α1 and α2 genes. Selective IgAD patients showed no α1 or α2 mRNA expression and extremely low protein levels, while secondary IgAD patients showed both mRNA and protein expressions of IgA subclasses. Partial IgAD can be classified into 3 patterns as follows: cases showing reduced levels of α1 and α2 gene expression; cases showing no α1 gene expression but normal α2 gene expression; and cases showing no α1 or α2 gene expression.

It is sometimes difficult to determine the pathogenic mechanisms operative in IgAD patients on the basis of serum IgA levels. Variations in the pathogenesis of IgAD patients might become better understood by examining the protein and mRNA expression levels of IgA subclasses.

ACKNOWLEDGEMENTS

This study was partly supported by a grant from the Ministry of Health, Labour and Welfare of Japan.

REFERENCES

1. Kerr MA. The structure and function of human IgA. *Biochem J* 1990;**271**:285-96.
2. Cunningham-Rundles C. Physiology of IgA and IgA deficiency. *J Clin Immunol* 2001;**21**:303-9.
3. Hammarstrom L, Vorechovsky I, Webster D. Selective IgA deficiency and common variable immunodeficiency. *Clin Exp Immunol* 2000;**120**:225-31.
4. Schaffer FM, Monteiro RC, Volanakis JE, Cooper MD. IgA deficiency. *Immunodefic Rev* 1991;**3**:15-44.
5. Bottaro A, de Marchi M, de Lange GG, Carbonara AO. Gene deletions in the human immunoglobulin heavy chain constant region gene cluster. *Exp Clin Immunogenet* 1989;**6**:55-9.
6. Lefranc MP, Hammarstrom L, Smith CI, Lefranc G. Gene deletions in the human immunoglobulin heavy chain constant region locus: molecular and immunological analysis. *Immunodefic Rev* 1991;**2**:265-81.
7. Plebani A, Carbonara AO, Bottaro A *et al.* Gene deletion as cause of associated deficiency of IgA1, IgG2, IgG4 and IgE. *Immunodeficiency* 1993;**4**:245-8.
8. Terada T, Kaneko H, Li AL *et al.* Analysis of Ig subclass deficiency: First reported case of IgG2, IgG4, and IgA deficiency caused by deletion of Cα1, ΨCγ, Cγ2, Cγ4 and Cε in a Mongoloid patient. *J Allergy Clin Immunol* 2001;**108**: 602-6.
9. Islam KB, Baskin B, Nilsson L, Hammarstrom L, Sideras P, Smith CI. Molecular analysis of IgA deficiency. *J Immunol* 1994;**152**:1442-52.
10. Asano T, Kaneko H, Terada T *et al.* Molecular analysis of B-cell differentiation in selective or partial IgA deficiency. *Clin Exp Immunol* 2004;**136**:284-90.
11. Husain Z, Holodick N, Day C, Szvmanski I, Alper CA. Increased apoptosis of CD20$^+$IgA$^+$B cells is the basis for IgA deficiency: The molecular mechanism for correction in vivo by IL-10 and CD40L. *J Clin Immunol* 2006;**26**:113-25.
12. Salzer U, Chapel HM, Webster ADB *et al.* Mutations in TNFRSF13B encoding TACI are associated with common variable immunodeficiency in humans. *Nat Genet* 2005; **37**:820-8.
13. Castigli E, Wilson SA, Garibyan L *et al.* TACI is mutant in common variable immunodeficiency and IgA deficiency. *Nat Genet* 2005;**37**:829-34.
14. Flanagan JG, Lefranc MP, Rabbitts TH. Mechanisms of divergence and convergence of the human immunoglobulin alpha 1 and alpha 2 constant region gene sequences. *Cell* 1984;**36**:681-8.
15. Chintalacharuvu KR, Raines M, Morrison SL. Divergence of human α-chain constant region gene sequences. *J Immunol* 1994;**152**:5299-304.
16. Kondo N, Fukutomi O, Agata H *et al.* The role of T lymphocytes in patients with food-sensitive atopic dermatitis. *J Allergy Clin Immunol* 1993;**91**:658-68.
17. Stavnezer J. Immunoglobulin class switching. *Curr Opini Immunol* 1996;**8**:199-205.
18. Klasen IS, Goertz JH, van de Wiel GA, Weemaes CM, van der Meer JW, Drenth JP. Hyper-immunoglobulin A in the hyperimmunoglobulinemia D syndrome. *Clin Diagn Lab Immunol* 2001;**8**:58-61.
19. Camacho MT, Outschoorn I, Echevarria C *et al.* Distribution of IgA subclass response to *Coxiella burnetii* in patients with acute and chronic Q fever. *Clin Immunol Immunopathol* 1998;**88**:80-3.
20. Park SR, Kim HA, Chun SK, Park JB, Kim PH. Mechanisms underlying the effects of LPS and activation-induced cytidine deaminase on IgA isotype expression. *Mol Cells* 2005;**19**:445-51.
21. Islam KB, Nilsson L, Sideras P, Hammarstrom L, Smith CI. TGF beta-1 induces germ-line transcripts of both IgA subclasses in human B lymphocytes. *Int Immunol* 1991;**3**: 1099-106.
22. Nilsson L, Islam KB, Olafsson O *et al.* Structure of TGF-beta 1-induced human immunogloblin C alpha 1 and alpha 2 germ-line transcripts. *Int Immunol* 1991;**3**:1107-15.
23. Kitani A, Strober W. Differential regulation of Cα1 and Cα2 germ-line and mature mRNA transcripts in human peripheral blood B cells. *J Immunol* 1994;**153**:1466-77.
24. Hummelshoj L, Ryder LP, Nielsen LK, Nielsen CH, Poulsen LK. Class switch recombination in selective IgA-deficient subjects. *Clin Exp Immunol* 2006;**144**:458-66.
25. Beard LJ, Ferrante A. IgG4 deficiency in IgA-deficient patients. *Pediatr Infect Dis J* 1989;**8**:705-9.
26. Brusco A, Saviozzi S, Cinque F, Bottaro A, DeMarchi M. A recurrent breakpoint in the most common deletion of the Ig heavy chain locus (del A1-GP-G2-G4-E). *J Immunol* 1999;**163**:4392-8.
27. Plebani A, Ugazio AG, Monafo V, Burgio GR. Clinical heterogeneity and reversibility of selective immunoglobulin A deficiency in 80 children. *Lancet* 1986;**1**:829-31.
28. Kawai T, Iida Y, Kojima Y *et al. [Normal value of laboratory examination in Japanese pediatric practice].* Tokyo: Japan Public Health Association, 1996 (in Japanese).

Genetic alterations in medulloblastoma from mice with defective DNA double strand break repair.

Pierre-Olivier Frappart[1+], Youngsoo Lee[1+], Helen R. Russell[1], Nader Chalhoub[2], Michael Wang[3], Kenji Orii[1,4], Jayne Lamont[1], Jingfeng Zhao, Naomi Kondo[4], Suzanne J. Baker[2] and Peter J. McKinnon[1]*

[1]Department of Genetics & Tumor Cell Biology, [2]Department of Developmental Neurobiology and [3]Hartwell Center for Biotechnology, St. Jude Children's Research Hospital, Memphis TN 38105, [4]Department of Pediatrics, Gifu University Graduate School of Medicine, Japan.

[+]These authors contributed equally to the manuscript,

*Corresponding author: Peter J. McKinnon

Department of Genetics and Tumor cell biology
332 N. Lauderdale Street, Memphis TN, 38105
Telephone: +001-901-495-4500
Fax: +001-901-526-2907
E-mail: peter.mckinnon@stjude.org

[Reviewers --Kevin Roth/Paul Hasty/Maria Jasin /Ramon Parsons.

Abstract

Inactivation of homologous recombination (HR) or non-homologous end-joining (NHEJ) predisposes to a spectrum of tumor types. Here, we have inactivated DNA double-strand break repair (DSBR) proteins, DNA Ligase IV (Lig4), Xrcc2 and Brca2 or combined Lig4/Xrcc2 during neural development using Nestin-cre. In all cases, inactivation of these repair factors, together with p53 loss, lead to rapid medulloblastoma formation. Genomic analysis of these tumors showed recurring chromosomal 13 alterations via chromosomal loss or translocations involving regions containing *Ptch1*. Sequence analysis of the remaining *Ptch1* allele showed a variety of inactivating mutations in all tumors analyzed, highlighting the critical tumor suppressor function of this hedgehog-signaling regulator. We also observed genomic amplification or upregulation of either N-Myc or cyclin D2 in all medulloblastomas. Additionally, Pten was also selectively targeted in tumors arising after disruption of HR. Thus, our data illustrate the central requirement for Ptch1 tumor suppressor activity in preventing medulloblastoma and reveal other fundamental events required for cerebellar granule cell transformation.

Introduction.

Repair of DNA double strand breaks (DSBs) can occur via non-homologous end joining (NHEJ) or homologous recombination (HR). A distinguishing feature between these pathways is the requirement of HR for a sister chromatid present in the S/G2 phase of replicating cells to provide an error-free template for DNA repair (1, 2). Multiple factors coordinate HR and amongst these, Xrcc2 and Brca2 are critical (3, 4). In contrast to HR, NHEJ is an error-prone repair mechanism that enzymatically modifies the two ends of a DNA break so that they are compatible for direct ligation (5-8). Of the factors important for NHEJ, a DNA ligase IV (Lig4)/Xrcc4 complex facilitates ligation of broken non-compatible DNA ends. During development of the central nervous system (CNS), HR is required for prevention of genomic instability in proliferative progenitor cells while NHEJ molecules are critical in post-mitotic neurons to maintain genomic integrity (9), and their inactivation can perturb development of the nervous system, leading to neurodegeneration, microcephaly or brain tumors (10).

Medulloblastoma is the most common malignant pediatric brain tumor, and often arises from the granule neuron progenitors (GNPs) in the external germinal layer (EGL) of the developing cerebellum (11, 12), and many medulloblastoma models have a very similar gene expression profile to GNPs (13-17). Several human syndromes, such as Turcot (*APC* germline mutation), Gorlin (*PTCH1* germline mutation), Fanconi anemia complementation group D1 (*BRCA2* germline mutation) or Nijmegen Breakage (*NBS1* hypomorphic mutation), predispose to medulloblastoma (12, 18, 19). Additionally, mutations of other genes involved in the sonic hedgehog (SHH) pathway such as *SUFU*, *SMOH* or the Wingless (*WNT*) pathway such as *AXIN1* or *β-CATENIN* have also been found in sporadic human medulloblastomas, highlighting the importance of these pathways for preventing cancer (20). Mutations of the p53 pathway also occur in many sporadic medulloblastomas (14, 21, 22).

Consistent with the above, 10%-15% of *Ptch1* heterozygote mice develop medulloblastoma by 8 months of age, an event that is associated with inactivation of the remaining *Ptch1* allele (23-25). Loss of *p53* or *Ptch2* significantly increases the incidence of medulloblastoma in *Ptch1*$^{+/-}$ mice (24, 26). Although p53-null mice are not predisposed to develop medulloblastoma (27, 28), *p53* loss is a prerequisite in many models of medulloblastoma (15-17, 26, 29-31). Similar radiation susceptibility in *Ptch1*$^{+/-}$ mice suggests that DNA damage in the cerebellum strongly predisposes to tumorigenesis (32). Inactivation of proteins involved in NHEJ such as Lig4, Xrcc4 and Ku80 or HR such as Xrcc2 or Brca2 also leads to medulloblastoma formation in a p53-deficient background (9, 30, 31, 33, 34).

In order to further examine the genesis of medulloblastoma, we used neural-specific inactivation of conditional mutants for DNA DSB repair with associated p53 inactivation. Remarkably, we found that *Ptch1* was specifically lost in all DNA repair-deficient medulloblastomas, and this involvement was also associated with limited other cytogenetic rearrangements that also underpinned these tumors. Therefore, Ptch1 tumor suppressor activity is uniquely required to prevent transformation in cerebellar granule neurons, perhaps by restraining replication stress associated with SHH signaling.

Results.

Medulloblastoma in DSBR deficient mice.

While germline inactivation of *DNA ligase IV (Lig4)*, *Xrcc4* or *Xrcc2* is lethal at mid or early gestation, coincident inactivation of *p53* rescues lethality, and promotes a spectrum of tumors by ten weeks of age including lymphoma and medulloblastoma (9, 14, 35, 36). In order to carefully evaluate medulloblastoma exclusive of lymphoma, we generated mice carrying

conditional *Lig4* and *Xrcc2* alleles that were inactivated in neural progenitor cells during development using *Nestin*-cre. We used *Xrcc2*, *Brca2* and *Lig4* mutants to compare the effects of disruption of the two mammalian DNA DSB repair pathways, NHEJ (*Lig4*) or HR (*Brca2* and *Xrcc2*). For clarity, we refer to $Lig4^{LoxP/LoxP}$;*Nestin-cre* mice as $Lig4^{Nes\text{-}Cre}$ and have used a similar nomenclature for *Xrcc2* and *Brca2* animals. While inactivation of many DNA DSB repair genes results in embryonic lethality, conditional deletion of these genes throughout the nervous system was compatible with animal survival. A notable feature of the conditional mutant animals was the lack of pronounced apoptosis typical after germline inactivation of these genes, and likely reflects developmental timing of cre expression (data not shown). However, deletion of Lig4 using Meox2-cre, which expresses in the epiblast cells, leads to similar neuraxis-wide apoptosis as germline Lig4 deletion (Lee et al., unpublished). Nestin-cre mediated deletion of the Lig4 binding protein Xrcc4 was also found to lack the neural apoptosis observed when this gene is deleted in the germline (31).

We monitored tumor formation in $Lig4^{Nes\text{-}Cre}$, $Xrcc2^{Nes\text{-}Cre}$ and $Lig4/Xrcc2^{Nes\text{-}Cre}$ mice, whereby NHEJ, HR or both repair pathways were disrupted, and for each strain we analyzed co inactivation of p53 alleles. We observed tumor formation over a period of thirty-two weeks (Fig. 1A-C). We found that $Lig4^{Nes\text{-}Cre}$, $Xrcc2^{Nes\text{-}Cre}$ and $Lig4/Xrcc2^{Nes\text{-}Cre}$ mice developed medulloblastomas between 14 and 16 weeks of age when *p53* was also inactivated (Fig. 1A-C, Table 1). Additionally, *p53* heterozygosity only promoted medulloblastomas in $(Lig4;Xrcc2)^{Nes\text{-}Cre}$ mice, compared with either DNA repair mutant alone, with a tumor onset around 22 weeks of age (Fig. 1). We determined p53 status in medulloblastoma from the $(Lig4;Xrcc2)^{Nes\text{-}Cre};p53^{+/-}$ mice. To do this we performed aCGH and real-time PCR analysis and found that the WT *p53* allele was lost (Fig.1D-E), implying that *p53* loss of heterozygosity (LOH) contributed to medulloblastoma probably reflecting increased genomic instability when both repair pathways are inactivated. For comparison to the *Lig4* and *Xrcc2*-

deficient mice, we also compared *Brca2*$^{Nes\text{-}Cre}$;*p53*$^{-/-}$ mice which also rapidly develop medulloblastoma (33), as do *Brca2*$^{Nes\text{-}cre}$;*p53*$^{+/-}$ also via inactivation of the wild type (WT) *p53* allele (Fig. 1D).

Defective DNA DSB repair leads to specific inactivation of Ptch1.

Multiple medulloblastomas from each of the different repair mutants were analyzed using aCGH and spectral karyotyping (SKY). We detected chromosome 13 alterations as a common event in medulloblastoma using aCGH, and this involved lost or translocation of one copy of chromosome 13 (Fig. 2A-C, suppl. Table 1). Analysis of the region of chr13 involved in the translocations using BAC clone assignments revealed that in all cases it involved *Ptch1*, suggesting that *Ptch1* inactivation was a key target in medulloblastoma formation. Because one copy of *Ptch1* was inactivated through chromosome loss or translocation, we determined the status of the remaining *Ptch1* allele. To do this we sequenced *Ptch1* mRNA via cDNA amplification and found mutations in the remaining *Ptch1* allele in all tumors analyzed (n=20; Fig. 2D, Suppl. Table 2). In most cases, these mutations lead to a truncated Ptch1 protein that would inactivate Ptch1 or substantially affect function. To confirm that these were *bonafide* tumor-related *Ptch1* mutations, which arose from genomic mutation, we sequenced the corresponding regions of genomic DNA. We found that in all cases genomic DNA from the tumors contained the corresponding mutation found in the cDNA. For example, splice donor/acceptor mutations were found that would predict exon skipping, as observed in the tumor-derived *Ptch1* cDNA. We also confirmed that inactivation of *Ptch1* was central to tumor formation by evaluating tumor latency and *Ptch1* status in *Ptch1*$^{+/-}$ compound mutants. We also generated *Brca2*$^{Nes\text{-}Cre}$;*Ptch1*$^{+/-}$;*p53*$^{+/-}$ (or *p53*$^{-/-}$) mice and compared tumor latency between various related genotypes (Suppl. Fig. 1). Latency was dramatically reduced (<5 weeks) in *Brca2*$^{Nes\text{-}Cre}$;*Ptch1*$^{+/-}$;*p53*$^{-/-}$ mice and aCGH or SKY

analysis of the resulting tumors showed loss of the remaining WT *Ptch1* allele, (and also *p53* in the case of *Brca2*$^{Nes\text{-}Cre}$;*Ptch1*$^{+/-}$;*p53*$^{+/-}$) (Supplementary Fig. 4). These data indicate that loss of *Ptch1* is closely linked to the genesis of medulloblastoma.

Ptch1 functions to modulate smoothened activation of Gli factor transcriptional activity (37). Consistent with Ptch1 inactivation, activation of the SHH pathway was found in all medulloblastomas analyzed (n=16; Fig. 3A). A similar gene expression profile occurred in all medulloblastomas with upregulation of a common cohort of genes, including known target genes of the Shh-signaling pathway such as *Math1*, *sFrp1*, *Ptch2*, *Gli1*, *N-Myc*, *Sox18* and *D-Cyclins*. We also confirmed the microarray expression profile using real-time PCR in comparison with wild type or *p53*$^{-/-}$ P5 and adult cerebella (Fig. 3B). Together these data indicate that inactivation of DSB repair leads to LOH of *Ptch1* and activation of the Shh pathway.

N-Myc or Cyclin D2 are amplified in the DSB repair deficient medulloblastomas

While loss of chr13/Ptch1 was a defining event in all medulloblastoma, other recurring chromosomal changes were also present. These included amplification of regions of chr12 and chr6, corresponding to *N-Myc* and *Cyclin D2*, and more selectively, loss of a portion of chr19 in medulloblastoma associated with tumors arising in Brca2 mutants or after co-inactivation of Lig4 and Xrcc2 (Fig. 4). We found that the *N-Myc* locus was amplified on chr12 (localized on two BACs: RP23-10C3 and RP23-246B9) in medulloblastoma samples spanning all DNA repair mutant genotypes (Fig. 4A, E). In some cases, N-Myc amplification was reflected by abundant double minute chromosomes; we confirmed *N-Myc* amplification in those tumors using fluorescence *in situ* hybridization (FISH) and found a strong signal corresponding to multiple copies of N-Myc (Fig. 4C).

While *N-Myc* amplification was a prominent feature in medulloblastomas, tumors not showing genomic *N-Myc* alterations were often associated with an amplification of chr6, suggesting a reciprocal relationship between N-Myc and Cyclin D2 amplification. As Cyclin D2 is expressed at high levels in the medulloblastoma and is located on Chr6, we confirmed the involvement of cyclin-D2 in many of the $Brca2^{Nes\text{-}cre};p53^{-/-}$ tumors using aCGH to map the region of chr6 that was amplified (Fig. 4A, E) and Cyclin D2 FISH (data not shown). The chromosomal changes associated with these events probably augment initial mutations acquired by the tumor, however these genes also function as SHH targets, and this fact probably accounts for enhanced expression of N-Myc and Cyclin D2 in all tumors. Thus, *Ptch1* loss and subsequent upregulation of the SHH will also promote increased N-Myc and cyclinD2 expression as seen in Fig. 3. Either *N-Myc* or *Cyclin-D2* amplification during tumor progression would contribute to the evolution of the medulloblastoma by providing a potent growth advantage.

Defective homologous recombination targets chromosome 19.

Further analysis of the genetic changes present in medulloblastomas identified a loss of chr19, by either translocation or chromosome loss associated with tumors in which HR was disabled (Fig. 4D). We found that *Brca2*-deficient (19/25), *Xrcc2*-deficient (3/9) and *Ligase4*/*Xrcc2*-deficient tumors (4/5), but not *Lig4*-deficient tumors were associated with loss of chr19; a finding consistent with the presence of a tumor suppressor gene. The loss of chromosome 19 has also been reported in some other medulloblastoma models (17, 38). Known tumor suppressors on mouse chromosome 19 include *Pten* and *Sufu*. While *SUFU* loss has been directly linked to medulloblastoma, PTEN loss has recently been associated with defective BRCA1 in breast cancer (29, 39, 40). Therefore we examined if either of these two tumor suppressors were inactivated in our medulloblastoma models. Although the *Sufu*